Supporting material for: Viscous interfacial layer formation causes electroosmotic mobility reversal in monovalent electrolytes

Majid Rezaei,[1,2] Ahmad Reza Azimian,[1] Ahmad Reza Pishevar,[1] and Douwe Jan Bonthuis[2]

[1] *Department of Mechanical Engineering, Isfahan University of Technology, 8415683111 Isfahan, Iran*
[2] *Fachbereich Physik, Freie Universität Berlin, 14195 Berlin, Germany**

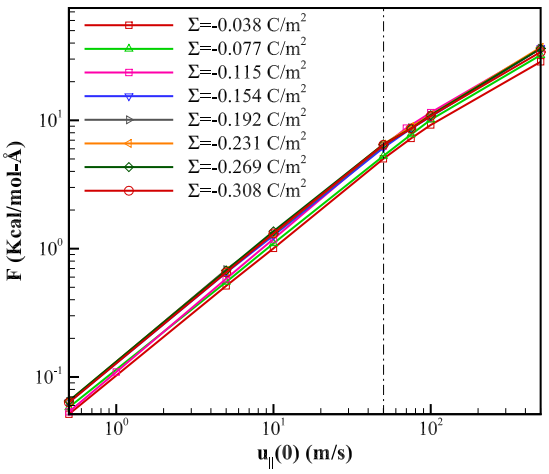

Figure 1. The friction force F as a function of the shear velocity $u_{\parallel}(0)$ for the case with differen surface charge densities

1. List of simulations

Table 1 shows a summary of the simulations implemented in the present work.

2. The linear friction regime

In the linear friction regime, the linear shear friction coefficient $\gamma = \frac{F}{Au_{\parallel}(0)}$, which is the friction force divided by the shear velocity $u_{\parallel}(0)$ and the area A, is constant [1].

In the present work, all the shearing simulations are performed in the linear friction regime by setting the shear velocity to $u_{\parallel}(0) = \pm 50\ \frac{m}{s}$, where the friction force is still a linear function of the shear velocity (see Fig. 1), resulting in a shear friction coefficient which is independent of the shear velocity.

3. Effect of different parameters on the mobility variations

Figure 2 shows the variation of the electroosmotic mobility as a function of the surface charge density for the cases simulated under different conditions. We first check the linearity of the electrokinetic response as a function of the strength of the applied electric field. As a function of the electric field strength, the electroosmotic mobility increases, which is caused by extension of the double layer width under influence of the hydrodynamic lift force [2]. This nonlinear effect is not expected to be observed in experiments, because the electric field strength used is typically significantly lower. The electric field strength used in this study is just outside the linear regime.

From Fig. 2, we extract the values of Σ_{opt} and Σ_{rev} for all different simulation systems, the results of which are shown in Fig. 5 of the main text. Σ_{inv} and the IHL onset are calculated directly from the charge distributions.

4. The integrated charge densities in the Helmholtz layer for the different system parameters

Figure 3 shows dependence of the surface charge that is neutralized by the Helmholtz layer on different parameters. Here, what we mean by the Helmholtz layer is the combination of both the inner and the outer Helmholtz layers. This figure is used for calculation of the charge inversion surface charge density (the red curves shown in Fig. 5 in the main text). This figure also could be used to detect the surface charge density at which half of the surface charge becomes neutralized by the outer Helmholtz layer, which for the standard system coincides with the optimum surface charge density where the electroosmotic mobility is maximum. Note that at low surface charges, where half or less of the surface charge is neutralized by the Helmholtz layer, the surface electrostatic forces are not strong enough to form a charged inner Helmholtz layer (see Fig. 5 in the main text), meaning that the total charge of the Helmholtz layer is confined to the outer Helmholtz layer.

5. The potential of mean force at zero surface charge

The potential of mean force, $V_{\pm}$, which is a non-electrostatic contribution to the potential, can be calculated as

$$V_{\pm}(z) = -ln(\frac{c_{\pm}(z)}{c_0}) \tag{1}$$

where $c_{\pm}$ is the concentration of positive and negative ions, and c_0 is the ion concentration in the channel center. As mentioned in the main text, the purely repulsive potential of mean force at $\Sigma = 0$ (see Fig. 4) reveals that charge inversion in this system occurs in the absence of non-electrostatic attraction.

Table I. List of simulations

	$\lvert\Sigma(C/m^2)\rvert$	$E_\parallel(V/nm)$	$\epsilon_{Na+}(cal/mol)$	$\sigma_{Na+}(nm)$	$\epsilon_{Si}(cal/mol)$	N_{Cl-}	$\phi_q(\%)$	$u_\parallel(0)$
1. Standard EOF simulations	0-0.308	0.55	14.8	0.258	584	80	100	0
2. $E_\parallel$ variations	0-0.308	0-1	14.8	0.258	584	80	100	0
3. ϵ_{Na+} variations	0-0.308	0.55	14.8-800	0.258	584	80	100	0
4. σ_{Na+} variations	0-0.308	0.55	14.8	0.258-0.372	584	80	100	0
5. ϵ_{Si} variations	0-0.308	0.55	14.8	0.258	100-584	80	100	0
6. N_{Cl-} variations	0-0.308	0.55	14.8	0.258	584	0-80	100	0
7. ϕ_q variations	0-0.308	0.55	14.8	0.258	584	80	12.5-100	0
8. Shearing simulations	0-0.308	0	14.8	0.258	584	80	100	0-500
9. Zero surface charge simulation	0	0	14.8	0.258	584	80	100	0

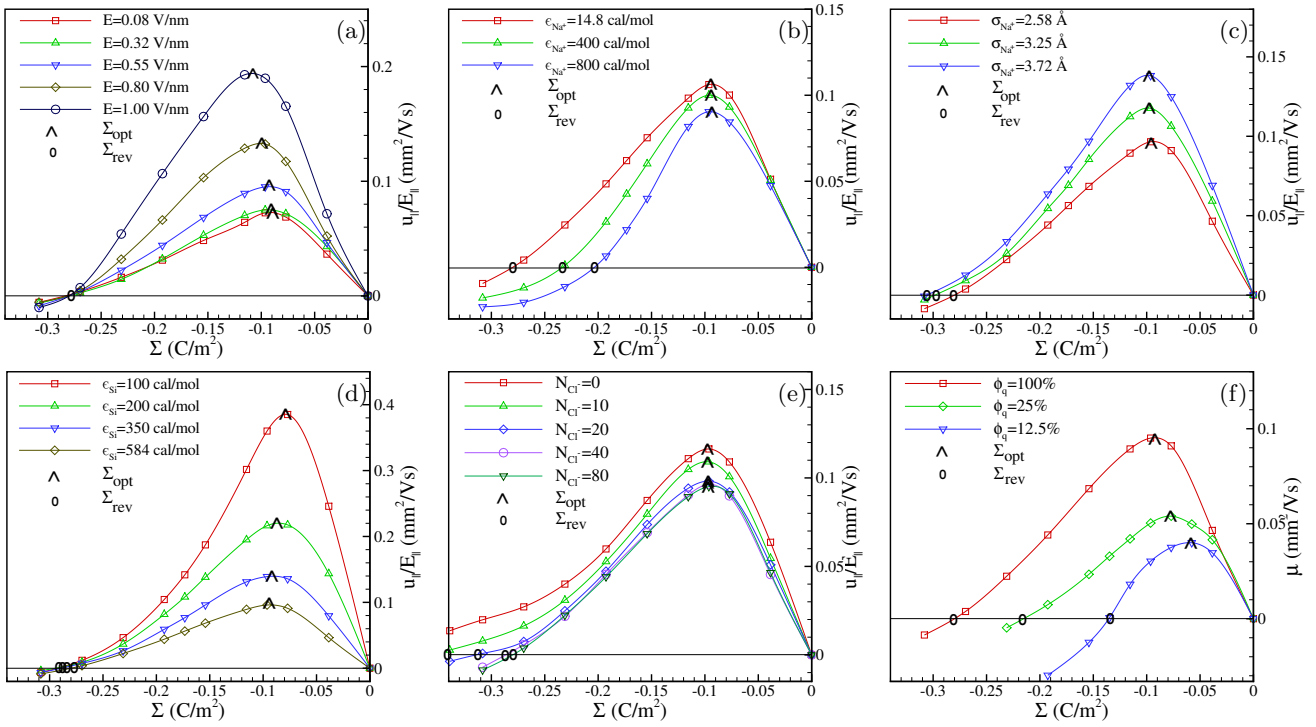

Figure 2. The electroosmotic mobility $u_\parallel/E_\parallel$ as a function of surface charge density Σ for the systems under different conditions made by changing (a) the external electric field strength $E_\parallel$; (b) sodium's depth of potential well ϵ_{Na+}; (c) sodium's Lennard-Jones size σ_{Na+}; (d) silicon's depth of potential well ϵ_{Si}; (e) the number of chlorides dissolved in the electrolyte solution N_{Cl-}; and (f) the percentage of the surface atomes which are electrically charged ϕ_q.

* Majid-rezaei@me.iut.ac.ir

[1] A. Schlaich, J. Kappler, and R. R. Netz, *Nano Letters*, 2017, **17**(10), 5969–5976.

[2] M. Rezaei, A. Azimian, and D. Toghraei, *Heat Mass Transfer*, 2015, **51**, 661–670.

[3] J. A. Lopez-Berganza, Y. Diao, S. Pamidighantam, and R. M. Espinosa-Marzal, *The Journal of Physical Chemistry A*, 2015, **119**(47), 11591–11600.

[4] S. Inaba and W. M. C. Sameera, *The Journal of Physical Chemistry A*, 2016, **120**(33), 6670–6676.

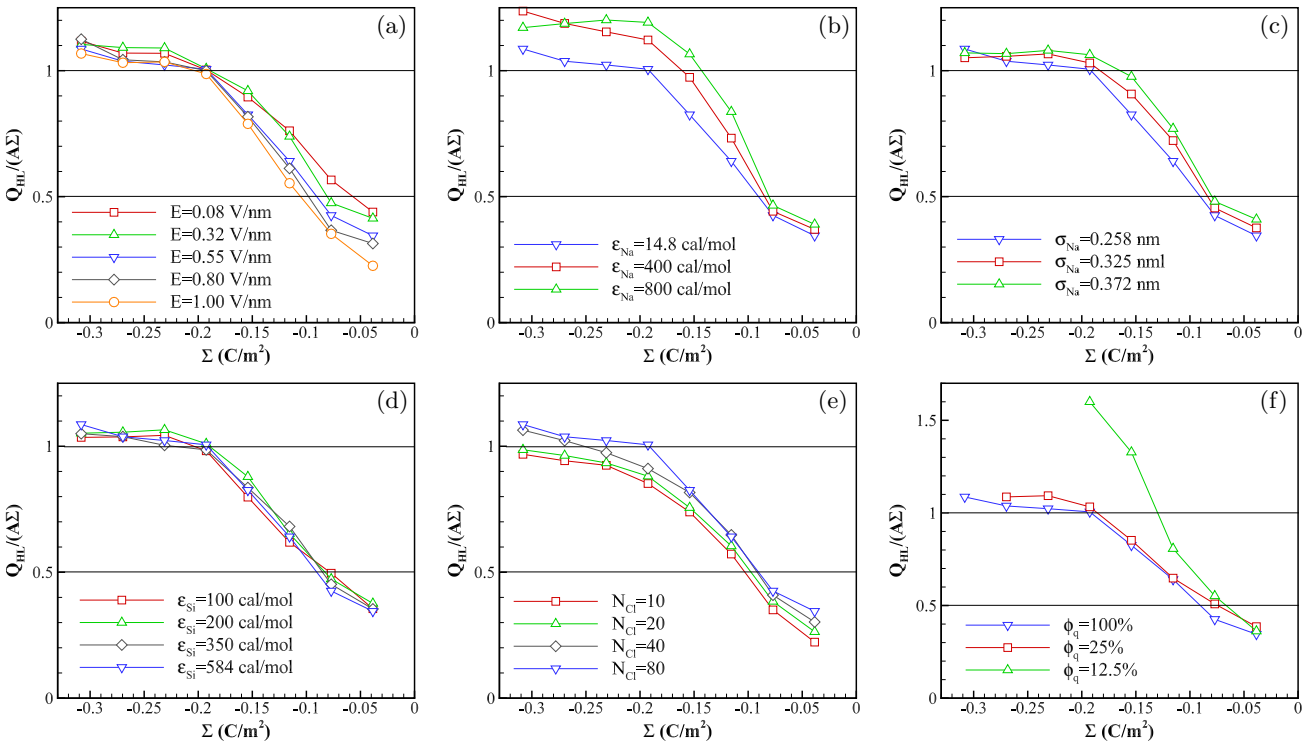

Figure 3. The integrated charge densities in the Helmholtz layer Q_{HL} as a function of surface charge density σ for the systems under different conditions made by changing a) the external electric field strength $E_{\parallel}$, b) sodium's depth of potential well ϵ_{Na^+}, c) sodium's Lennard-Jones size σ_{Na^+} d) silicon's depth of potential well ϵ_{Si}, e) number of chlorides dissolved in the electrolyte solution N_{Cl^-}, and f) percentage of the surface atomes which are electrically charged ϕ_q

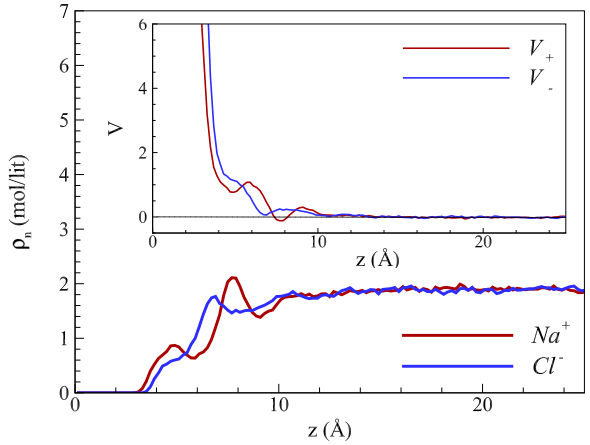

Figure 4. Ion number densities ρ_n and the resulted PMFs at zero surface charge density